SAND#
SAND2020-8499PE
PENDING

OPTICAL SPECTROSCOPY on Z MACHINE

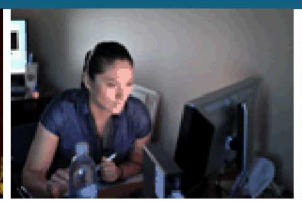

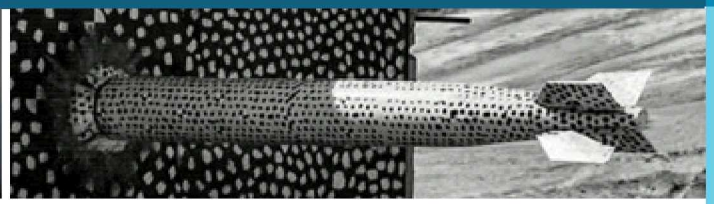

Presented by

Karin Fulford

Mentor: Sonal Patel

Manager: George Laity

01659, Advanced Capability for Pulsed Power

August 12, 2020

Presentation Outline

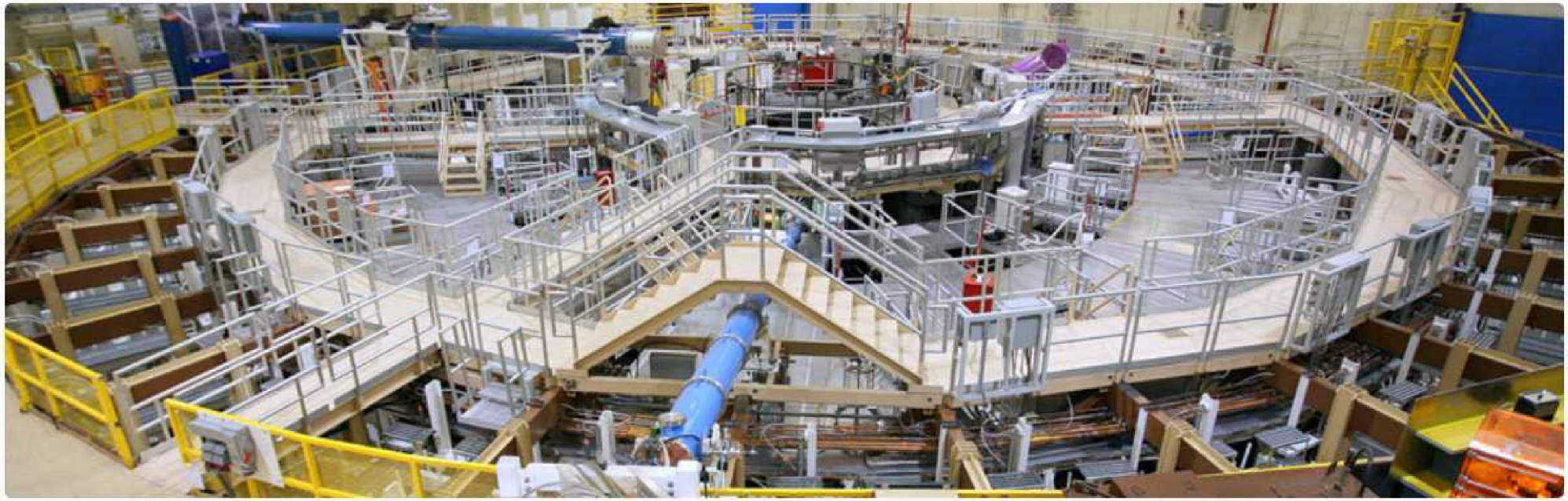

Source: https://www.sandia.gov/z-machine/research/energy.html

- ❑ **Z-division to Z Machine: A Few Historical Highlights**
- ❑ **Z Machine Overview**
- ❑ **Optical Spectroscopy on Z**
- ❑ **Calibration of Spectral Data**
- ❑ **The Project**

Z-division to Z Machine: A Few Historical Highlights

- Initiated by the Manhattan Project, the Z-division at Los Alamos National Laboratory (LANL), was an engineering cluster supporting nuclear efforts for US national security during WWII.
- The Z-division, along with weapons assembly and testing, moved from Los Alamos to Sandia Base during the mid-late 1940's.
- During this transition, Z-division engineers and military personnel banded to form Sandia Laboratory which quickly separated from LANL.
- Assigned by President Truman, AT&T became the managing contractor of Sandia Corporation.
- In 1946 the Atomic Energy Act introduced three civilian factions focused on stockpile stewardship:
  - Atomic Energy Commission (AEC)
  - Congressional Joint Committee on Atomic Energy
  - General Advisory Committee
- These entities embraced Sandia's efforts and ultimately laid a foundation for the current US Department of Energy (DOE), formed in 1977.

July 11, 1945. Sandia Base with military airfield in the foreground and developing laboratories in the back.

Source: Johnson, L. (1997).

Z-division to Z Machine: A Few Historical Highlights

- AEC established another nuclear design site in 1952 now known as Lawrence Livermore National Laboratory (LLNL). Along with LANL, this new California site would also focus on physics packaging design. From its continued collaboration with LLNL, Sandia established its California location in 1956, just blocks away from LLNL.
- In 1954, the AEC declared Sandia their Quality Assurance Agency for weapons materials, leading to a core value of high quality performance for the corporation.
- Sandia's workforce nearly doubled in ten years to almost 8,000 employees in 1962, but growth was temporarily halted by domestic and international efforts to limit nuclear investigations.
- Reduction in weapons development, along with energy shortages and terrorist concerns, led to beneficial collaborations and research diversification including energy sources, materials, seismic sensors, and radiation effects heading to pulsed-power studies.
- A significant advancement in pulsed-power was made in 1965 with the construction of HERMES, High-Energy Radiation Megavolt Electron Source. This success would lead to development of additional accelerators including HERMES II and III. The latter still currently in use for powerful gamma ray investigations.

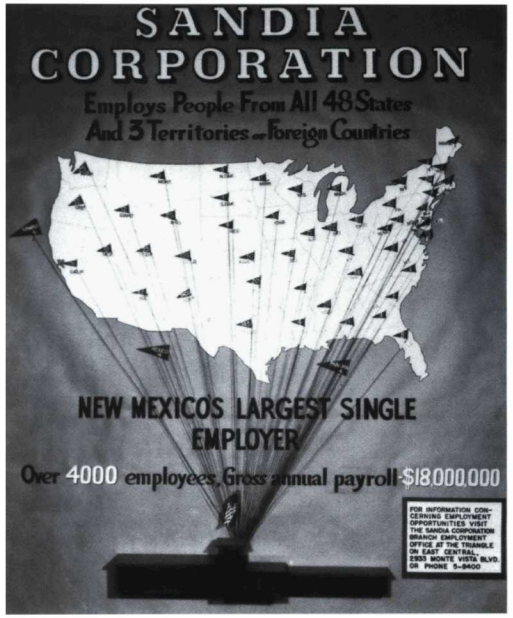

Top: 1950's workforce recruitment poster.

Bottom: HERMES II, in operation since 1968. Reconfigured to HERMES III in 1988.

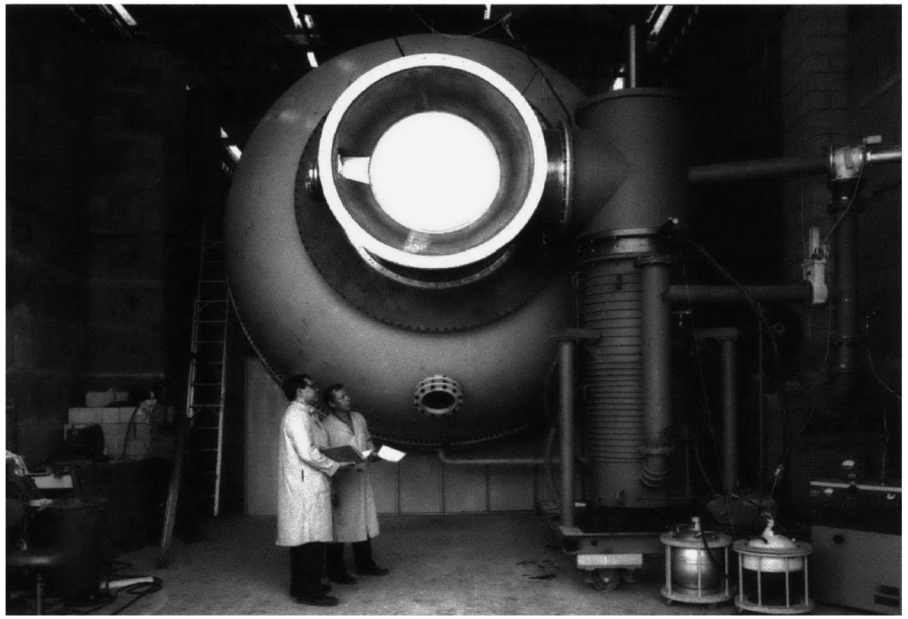

Source: Johnson, L. (1997).

Z-division to Z Machine: A Few Historical Highlights

- Throughout the 70s, 80s, and 90s, advancements in pulsed power and Inertial Confinement Fusion (ICF) led to the commission and reconfiguration of large accelerators. Namely, Particle Beam Fusion Accelerator II (PBFA II), operating in 1986, was reconfigured to expand radiation studies and became the Z Machine by 1996.
- In 2000, the Z Fundamental Science Program was introduced to invite academic collaborations and explore new plasma concepts and/or new material designs. That same year, the National Nuclear Security Administration (NNSA) was created under the DOE and is currently a primary funder of Z experiments to support questions concerning radiation effects and stockpile stewardship.
- From 2006-2007, Z was refurbished (project ZR) to improve switch reliability and increase energy storage providing 26 MA of current to a target. Since ZR, experiments on Z have been continuous, and focused on topics such as ICF, Dynamic Materials Properties (DMP), High Energy Density (HED), and X-ray radiation science.

Source: https://twitter.com/nnsanews/status/981883799062630400

Left: 1980 PBFA II in progress, later to become the Z Machine in 1996.

Right: Z Machine (pre-ZR), ~33meter diameter, displays power leakage through water insulated switches during a high current shot.

Sources:
- Van Arsdall, A. (2007).
- Sinars, D.B., et al. (2020).
- https://www.energy.gov/nnsa/about-nnsa

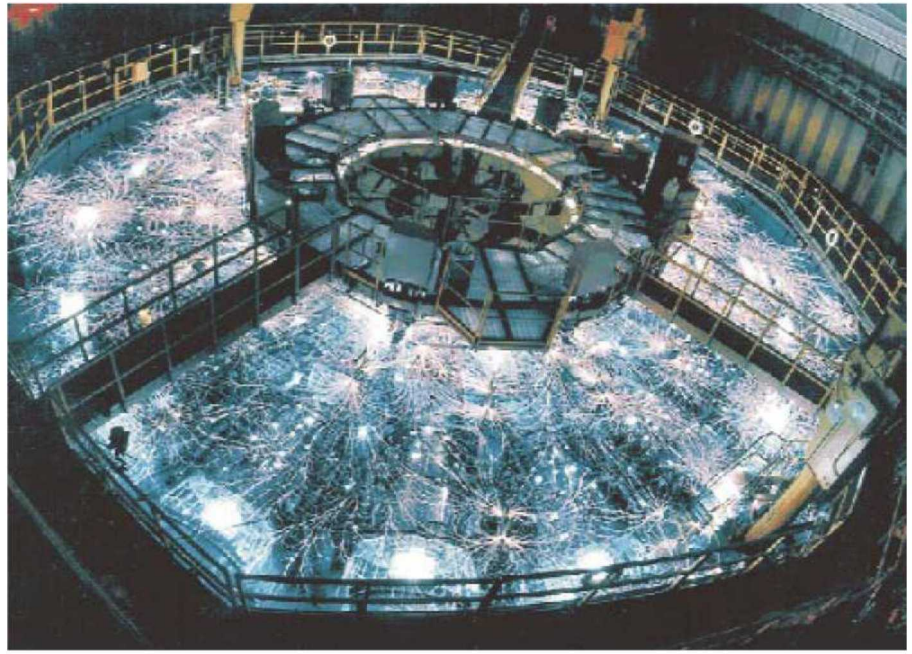

Source: Schwarzschild, B. (2003).

Z Machine Overview

- The Z complex is located in tech area IV where the Z machine is housed in building 983; encompassing nearly the entire building, as shown.
- Supplemental facilities such as the target chambers and staging area, provide resources for experiment versatility and engineering advancements.
- Included in the staging area is Mykonos (built in 2012), a terawatt linear transformer driver (LTD) used to investigate modular cavity performance for next-generation accelerators using advanced LTD switches.
- The Z-Backlighter facility houses the Beamlet laser initially developed at LLNL. In 2001 the laser was moved and reconfigured to become Z-Beamlet. This laser aids in magnetic linear inertial fusion (MagLIF) and HED opacity studies where high temperatures and exceeding brightness are required to better understand elemental photon effects.

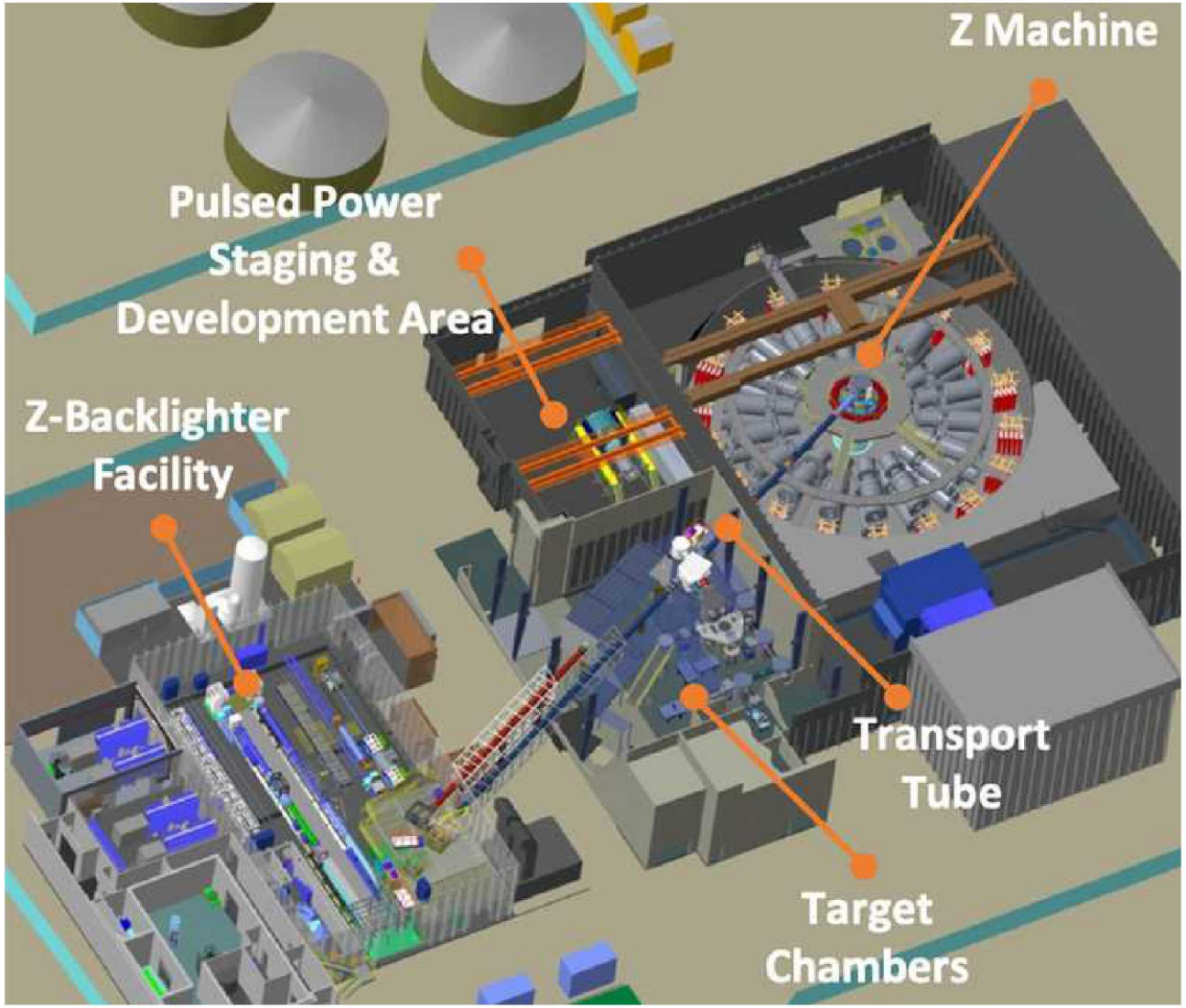

Illustration of Z complex, providing scale and proximity information of Z and supplemental amenities such as the Backlighter facility in building 986.

Sources: Sinars, D.B., et al. (2020). Schwarz, J., et al. (2017). Anderson, D., et al. (2012).

Z Machine Overview

- Evolving from ICF success on PBFA II, the transformation to Z involved the increase of z-pinch radiation sources to produce soft x-rays.
- Z-pinch scaling is achieved by passing energy through storage phases starting with Marx-generator capacitor banks.
- 36 generators make up this outer system where wall current flows to 60 capacitors for each generator. The megajoules of energy collected in generators can be released to the next storage section in about 1.3us. Peak current from each generator is ~180 kA.
- In the pulse forming stage, the energy is compressed in time through a low-inductance network of store capacitors, laser triggered gas switches, and transmission lines.
- Switch maintenance and performance is challenging to manage given the high voltage, high current, and precision demands.
- Self-closing water-insulated switches, rated for megavolt usage, are also used in the pulse forming stage. Primary concerns for these switches include jitter and resistive losses.

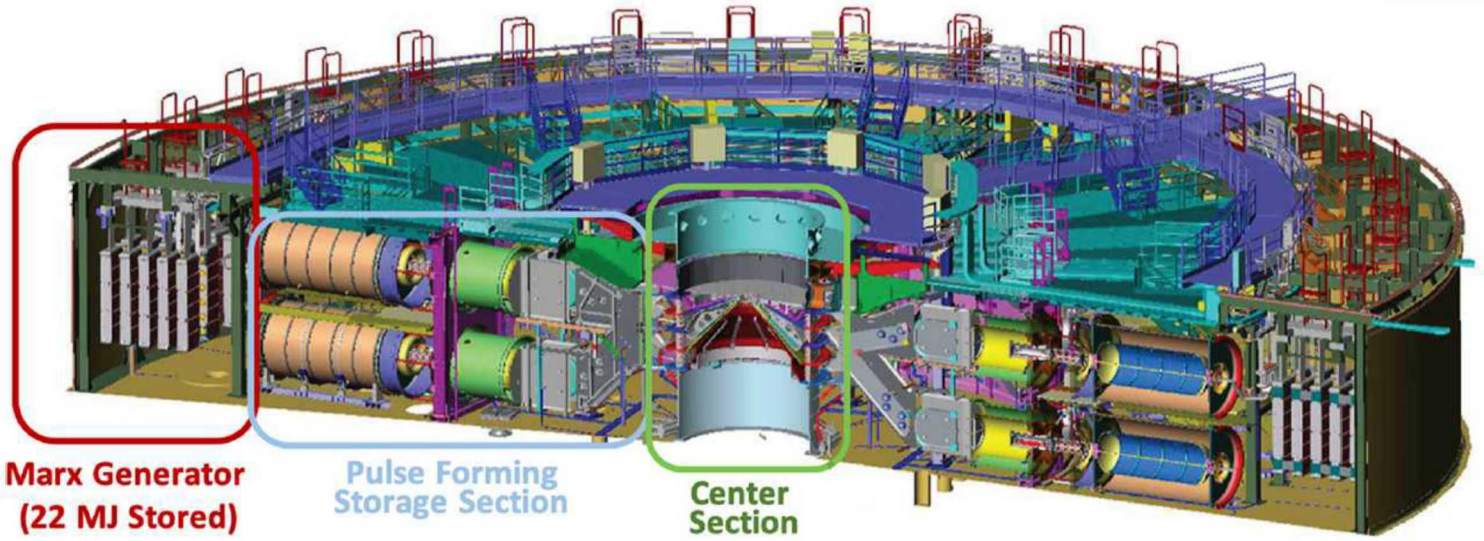

Cross section of the Z machine highlighting three key system stages, designed to compress energy in time and space to deliver mega amps of current to the center, producing extreme inward pressures exerted on the target.

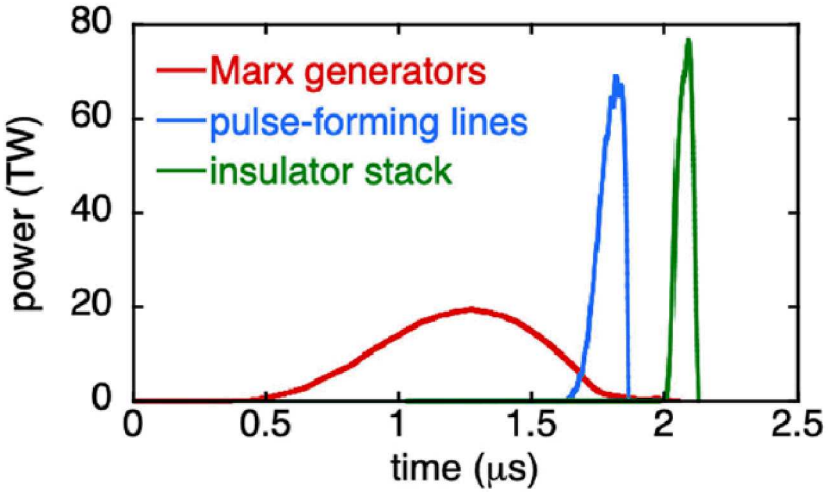

Graph illustrates how power is transformed during each stage of compression resulting in optimal power delivery to the center load.

Sources: Sinars, D.B., et al. (2020). Savage, M.E., et al. (2007).

Z Machine Overview

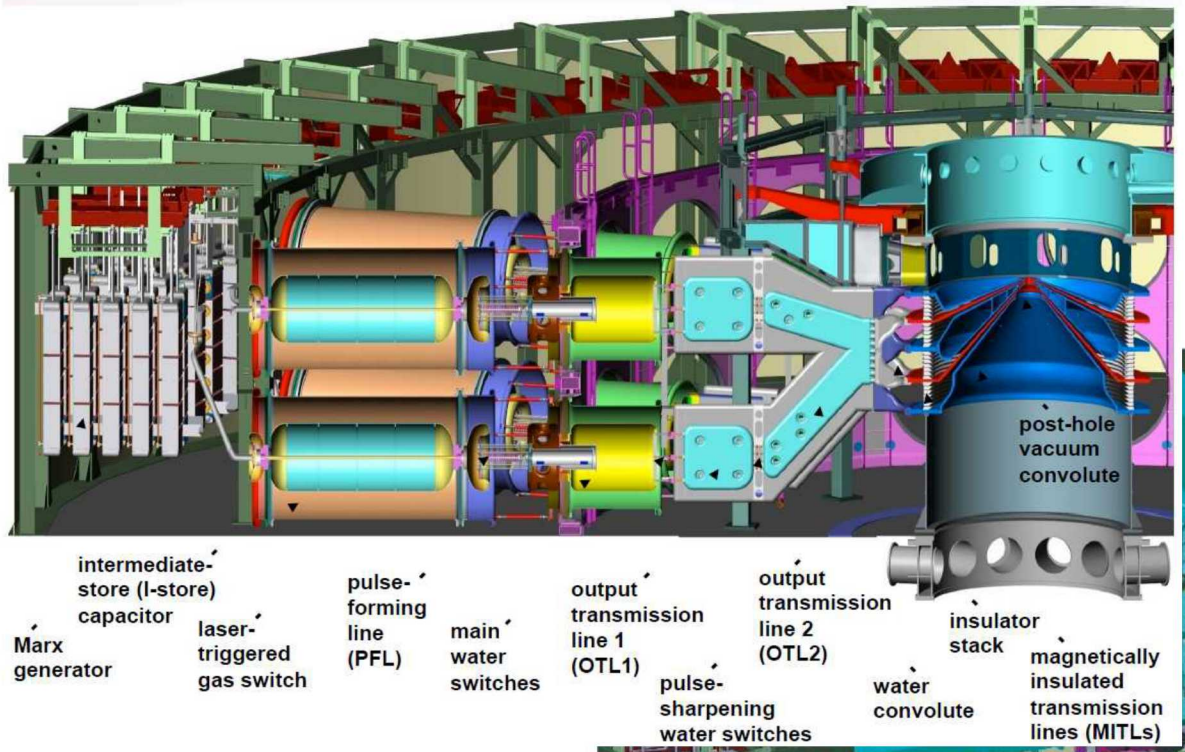

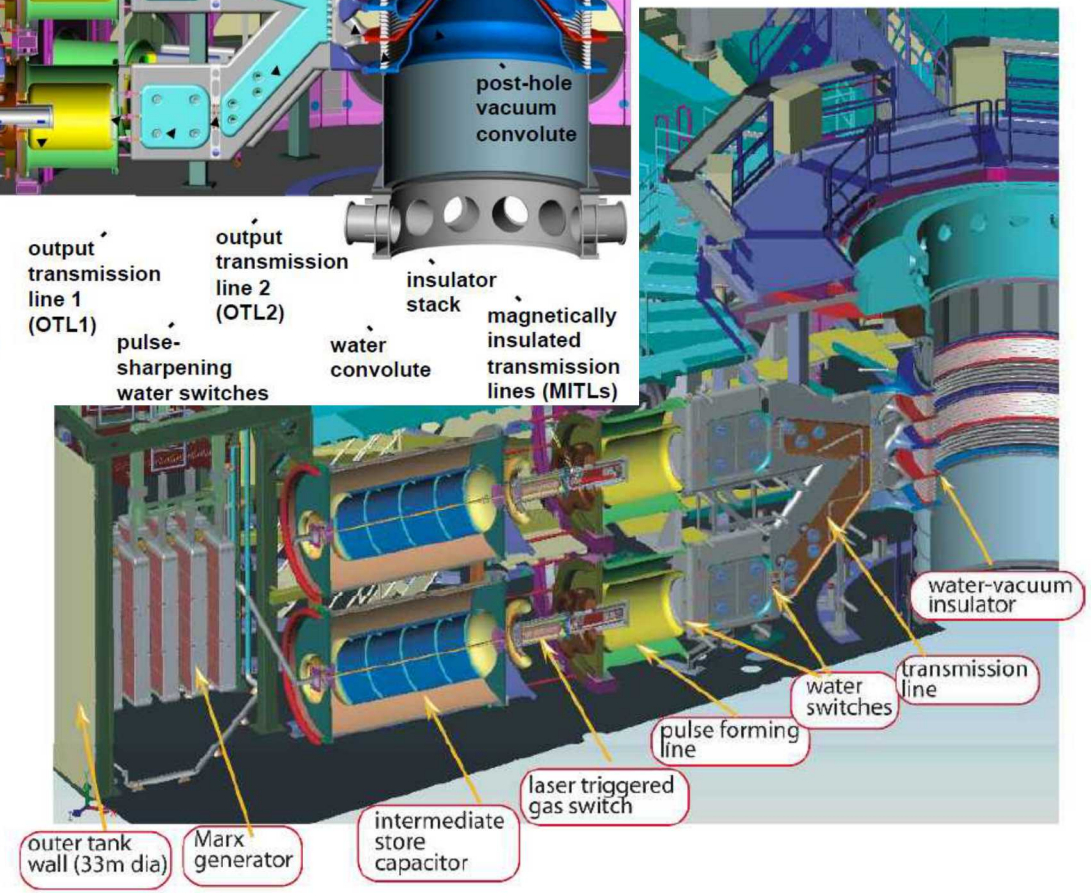

Two different views of Z machine details focused on the configuration of energy compression components.

Sources:
(Top) Anderson, D., et al. (2012) [Slide 4].
(Bottom image and content) Savage, M.E., et al. (2007).

- Power flows through water lines to a water convolute, transposing the electric field from horizontal to vertical at the center section.
- Further compression is achieved in the center section through 36 magnetically insulated transmission lines (MITLs) which can directly compress the energy up to 1us.
- The center section transitions to a vacuum environment requiring robust insulation efforts. As described by Savage, et al., in the load region, four insulator stacks are placed in parallel with the load positioned above the top insulator. Allowable flashover rate was determined to be 1% or less.
- Final feed to the load moves from MITLs to a double post-hole convolute. Plasmas are noted in this current combining region.

Z Machine Overview

- There are three basic categories of research performed on Z: basic science, applied science, and use-inspired.
- Relating the categories to the NNSA mission can be thought of this way:
  - Basic – new idea, weak mission
  - Applied – old idea, strong mission
  - Use-inspired – new idea, strong mission
- There are also three majority target types used on Z investigating plasma radiation sources, dynamic material properties, and magnetic direct drives.
- A wire-array radiation source has long evolved at Sandia to efficiently produce an imploding plasma generating soft x-rays. These studies support interpretation of stellar opacity data, improvements to spectral synthesis models, and knowledge of fundamental material properties.
- For DMP experiments, a "flyer plate" target, or planar geometry sample, is often used to examine sample impacts via JxB forces. Observed shock waves and/or compression results substantiate theoretical calculations for thermodynamics, transport, and strength properties.
- MagLIF studies, using direct laser heating (as shown), and ICF, using indirect x-ray heating, are focused fusion efforts on Z addressing magnetically increased containment for reaction stagnation and linear implosion stability physics, respectively.

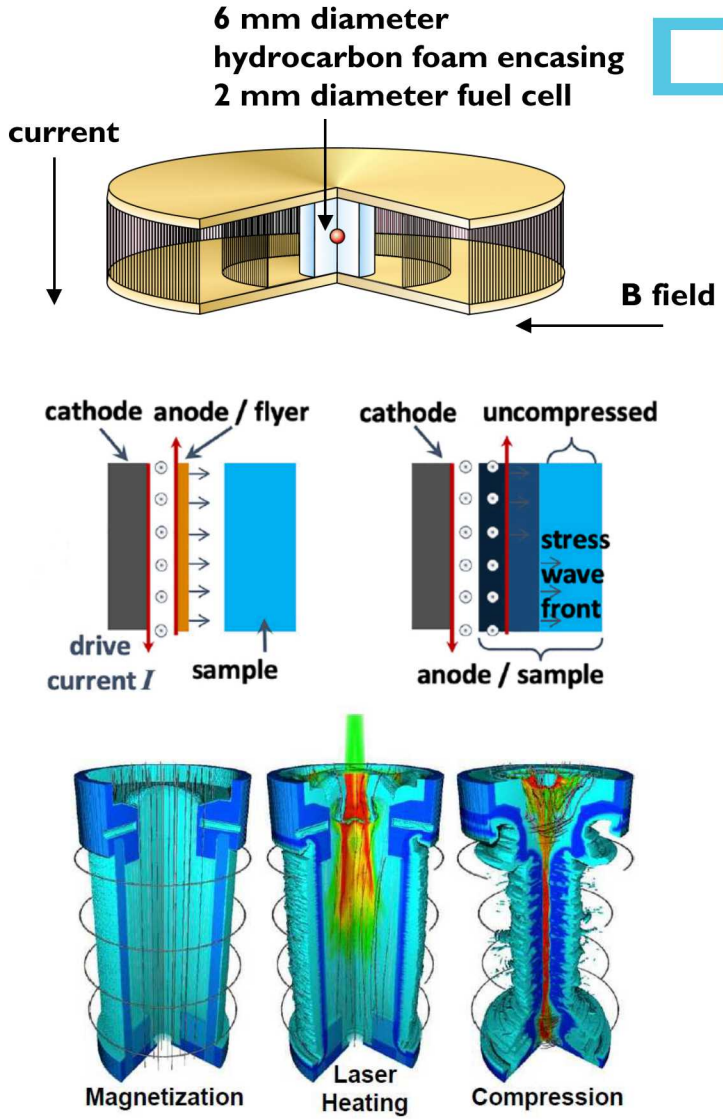

Three primary target types used on Z: wire-array for plasma radiation source (top), planar geometry sample with either shock or compression configurations (center), and magnetic direct fusion target (bottom) illustrating the three stage MagLIF process used to create a stagnant fusion conditions.

Sources: Schwarzschild, B. (2003). Anderson, D., et al. (2012). Sinars, D.B., et al. (2020).

Optical Spectroscopy on Z

- A primary goal for optical spectroscopy on Z is to gain insight into plasma formations that occur in the system during a shot event.
- As components quickly heat gases are released and particles ionize producing a variety of plasma formations with both high and low densities.
- While plasmas are often purposefully created to produce x-ray radiation, plasmas can also contribute to decreased efficiency and power loss delivered to the load on Z, hence one motivation to fully characterize these plasma occurrences.
- As presented by Cooper, plasma spectroscopy can be thought of as, "the study of electromagnetic radiation emitted from ionized media." Also affirmed, is the intrinsic link between radiator properties and plasma parameters.
- According to Cooper, there are at least three important spectral line broadening models in high temperature plasmas: natural, Doppler, and Stark (discussed on slide 15).
- Natural line broadening (Lorentz profile) depends on the lifetime of an excited state and is often negligible in lab plasmas.
- Doppler broadening (Gaussian profile) depends on the emitting species and its velocity distribution.

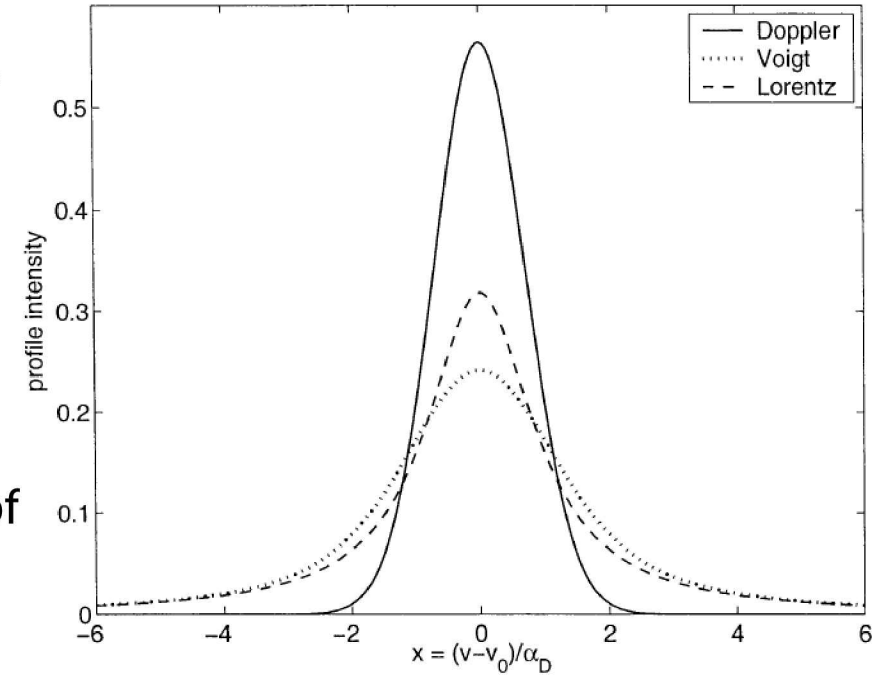

Illustration of line broadening models found in high temperature plasmas. Doppler equals Gaussian profile. Voight is the convolution of Gaussian and Lorentz. Source: Huang, X., & Yung, Y. L. (2004).

Sources: Cooper, J. (1966).

Optical Spectroscopy on Z

- Along with other feature diagnostics, such as B-dot and VISAR, many experiments on Z utilize optical spectroscopy to discern the presence or changes in an element from radiation exposure.
- As spectra characterization is know for each element, analysis of spectral data can produce time, spatial, and transformation information for an experimental event.
- While there are some limits to gathering full spectrum data, Streaked Visible Spectroscopy (SVS) is generally used for UV to visible range radiation.
- SVS employs streak cameras (streak tubes), electrically triggered, and fiber coupled to spectrometers.
- As shown, a streak tube passes light through a series of optics focused to a photocathode where electrons are sorted via high voltage sweeps toward the optional micro channel plate (MCP), see diagram comments.
- A phosphor screen converts electrons back to photons which produces the phosphor image.
- From the phosphor image intensity, wavelength, and time information are captured.

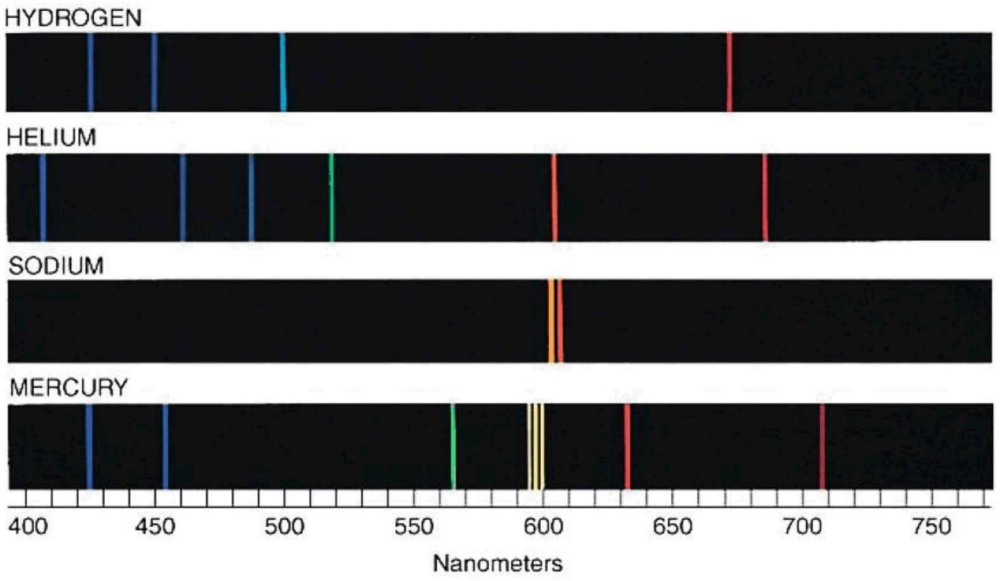

Above: Example of spectral characterization for a given elements.
Source: https://faculty.virginia.edu/skrutskie/images/light_spec_discrete.jpg

Below: Diagram of a streak tube illustrating the passage of light through a system to produce the phosphor image. MCP is used to amplify the signal but also increases noise, and is therefore an optional component.
Source: Hamamatsu Photonics K.K. (2008).

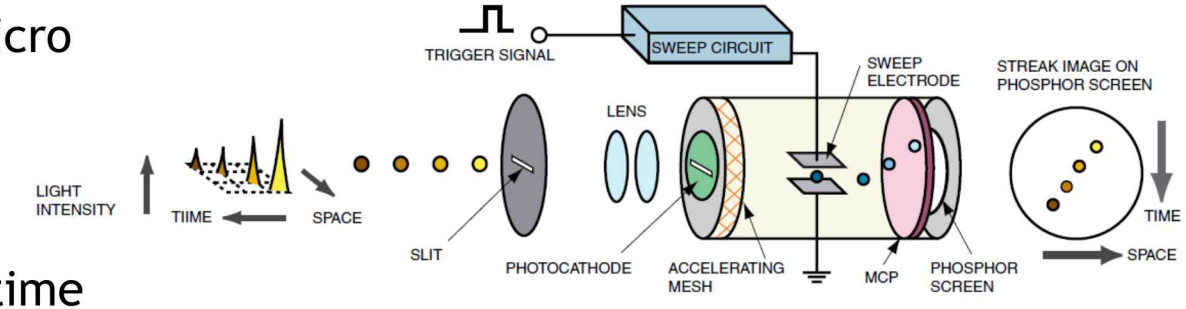

Optical Spectroscopy on Z

- As described, the streak camera records photon counts leading to intensity per wavelength per time ($W/m^2/nm/s$) data after calibration.
- Assuming a blackbody curve, surface temperatures can be calculated to approximate a plasma temperature.
- Temperature measurements can inform efforts for modeling and understanding current loss on Z.
- While data capture setups vary, a common setup for SVS is provided. The use of multiple cameras are used to capture same or difference information (e.g. wavelength regions, time, resolution) at different locations.
- There are currently four cameras available, two film and two digital. Due to challenges with film calibration, only the digital cameras are used for temperature measurements.
- Fiber optic runs between Z and the spectrometers is approximately 260'.
- To support timing and focus, the master trigger box houses an impulse generator, combs generator, and gate (voltage sweep).

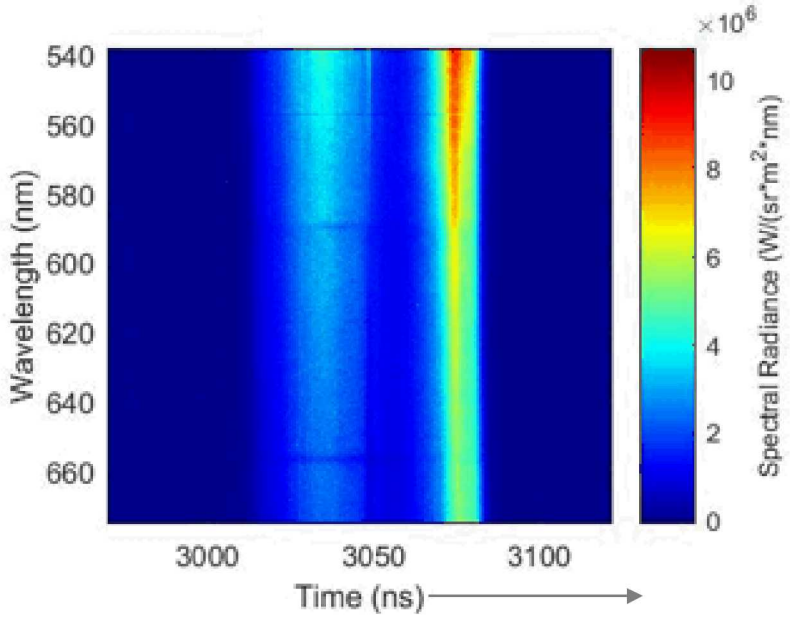

Above: Example of calibrated streak camera data.

Below: High-level diagram of typical SVS setup.

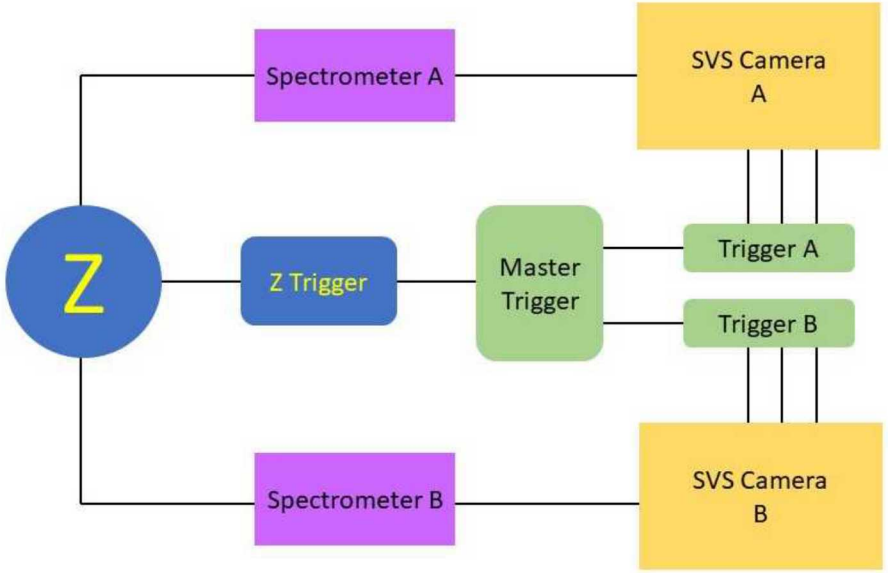

Optical Spectroscopy on Z

- The following published experiments are just a few examples of SVS information used for analysis of investigation findings:
  - ***Optical spectroscopy measurements of shock waves driven by intense z-pinch radiation***
    - Goals for this experiment included attaining temperature of a z-pinch driven shocked sample, spectra of dense plasma, and characteristics of shocked transparent window material.
    - Optical data from this study proved the ability to measure time-resolved spectra of shocked samples as well as capture spectra of dense warm plasmas. Additionally, line emissions observed at the window material indicate unexpected low density plasma formations, possibly due to adhesive.

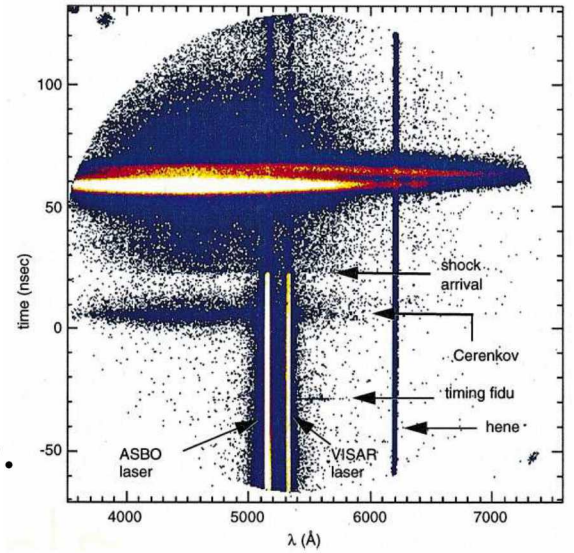

  - ***Magnetic field measurements via visible spectroscopy on the Z machine***
    - The goal of this experiment was to attain magnetic field measurements at a sodium doped Z target using SVS.
    - Spectral measurements and B-dot current measurements were compared to verify magnetic field magnitudes (>200 T) at current ~5 MA. Study led to identification of potential power loss between current probe and target.

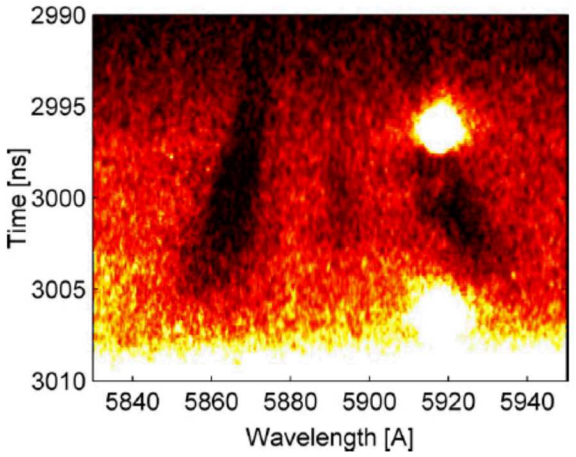

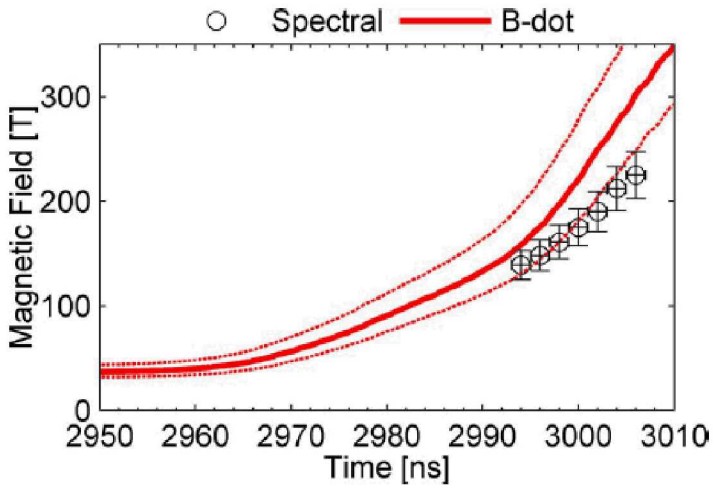

Sources: (top) Bailey, J. E., et al. (2000). (bottom) Gomez, M. R., et al. (2014).

Optical Spectroscopy on Z

- Additional published examples:

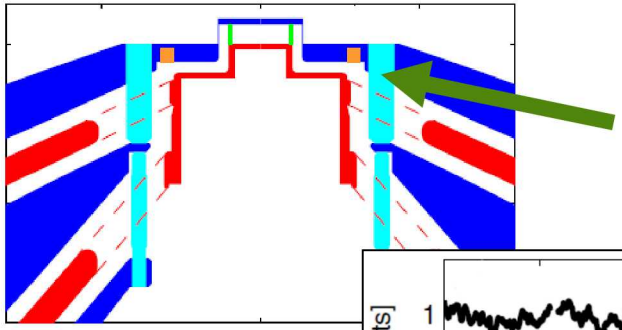

Post-hole convolute device (shown here in cyan) electrically connects transmission lines in the center section of Z.

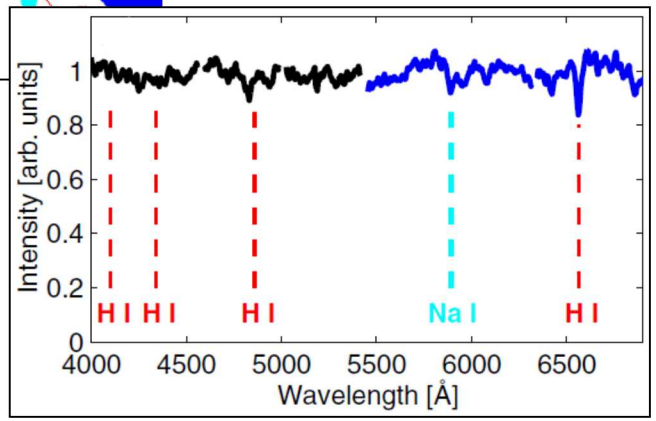

- ***Experimental study of current loss and plasma formation in the Z machine post-hole convolute***
  - Goals involved an in-depth evaluation of convolute current loss to improve simulations and improve convolute efficiency for design of future generators with exceeding currents.
  - For this study, optical data was collected from many experiments to encompass full visible spectrum observations. SVS data was used to deduce several plasma parameters such as location, density, temperature, and radial velocity.

- ***Active Dopant Optical Spectroscopy via Laser Ablation for High Resolution Spectral Measurements***
  [Sandia Report, Laboratory Directed Research and Development (LDRD)]
  - This work explored reliable use of laser ablated doping diagnostics, achieving high radiance on a stainless steel target doped with elements such as Li and Na. Example of Cu results are shown below.
  - SVS data was used to determine peak radiance levels and showed that low density emission lines can be measured from this technique. These results led to many suggestions for improved SVS efficiency on Z and will ultimately inform subsequent pulsed power developments.

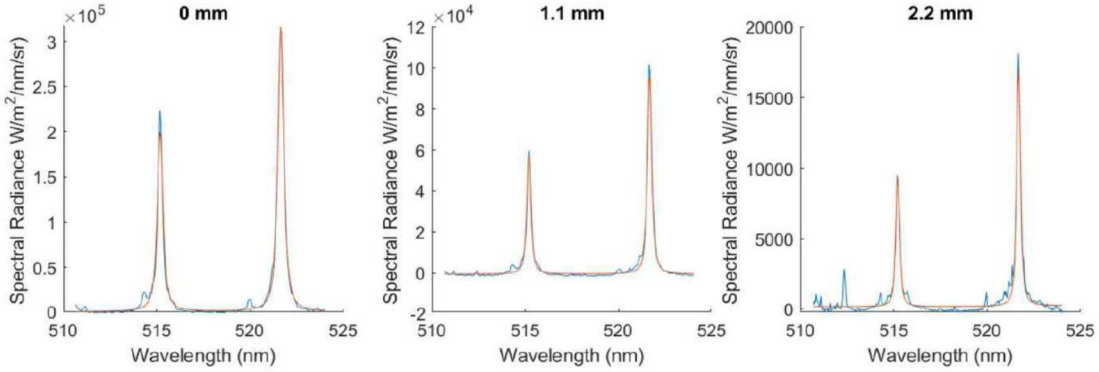

Sources: (top) Gomez, M. R., et al. (2017). (bottom) Patel, S., et al. (2019)

Optical Spectroscopy on Z

- Important effects observed from SVS:
  - Zeeman (weak field): splitting of spectral lines due to applied magnetic field
    - A: unmagnetized
      B: magnetized transverse splitting
      C: magnetized longitudinal splitting
    - As restated by Patel, three Zeeman rules exist:
      I. Line splitting is symmetric about the unshifted line for the weak and strong field cases (However, depending on the element, asymmetric line shifting can occur for the intermediate magnetic field case.)
      I. Sum of intensities at the split atomic level equal the sum of intensities in any Zeeman split level
      II. Unpolarized light must be the result from the combined components
    - Paschen-Back (strong field): splitting of atomic energy levels due to strong magnetic field
  - Stark broadening: splitting and shift of spectral lines due to macro and micro electric fields
    - Stark effect can be used to measure electron densities
    - Work in progress to measure electric fields

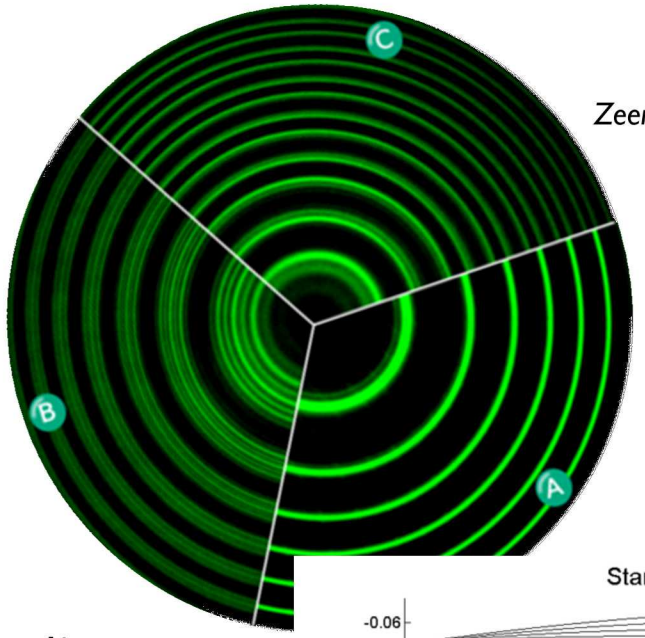

Zeeman Effect

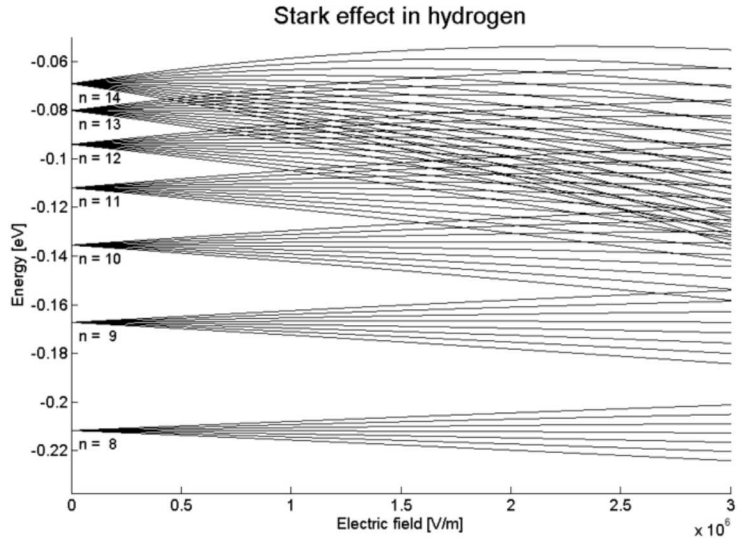

Source: Patel, S. (2016).

Top: Illustration of Zeeman splitting under magnetized and unmagnetized conditions.
Source: http://www.starkeffects.com/stark_effect.shtml

Bottom: Example of Stark effect, energy as a function of electric field for different quantum states.
Source: https://en.wikipedia.org/wiki/Zeeman_effect

Calibration of Spectral Data

- SVS systems on Z are calibrated using a tungsten source. In the SVS set up, Z is replaced with the cal source as achievable given instrument limitations. Weak tungsten radiance requires slow sweep (8 seconds) and corrections are performed to compare with Z data rates.
- A correction is constructed using a bright laser driven light source (LDLS). A ratio of fast/slow LDLS sweeps provides a nominal correction coefficient. The fast sweep is roughly 500 ns, and the slow sweep is 8 s.
- Due to the brightness of the LDLS, an ND filter is used to procure usable values and protect the camera during the 8 s sweep.
- This multistep process does produce an adequate correction for the tungsten source, but procedures are time consuming and introduce multiplied uncertainties including LDLS fluctuations for the longer sweeps.
- Additionally, while the tungsten source is extremely reliable, its limited flux and limited lower spectral range motivate investigations for alternative sources.

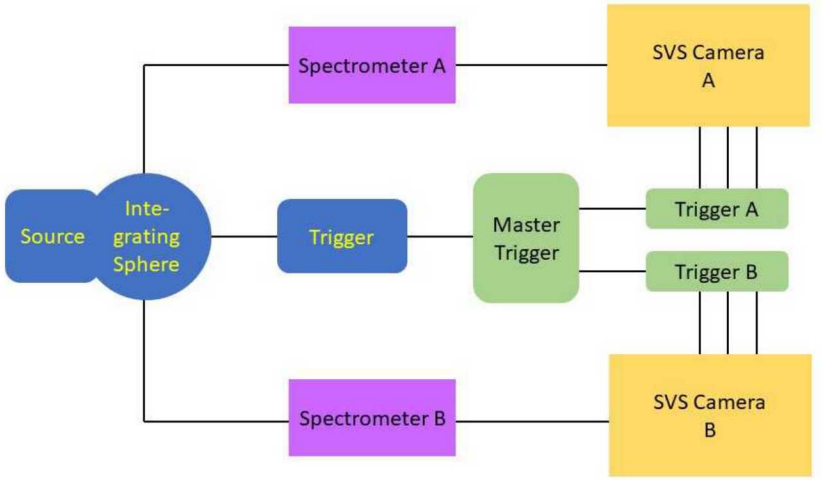

Sample of SVS calibration setup utilizing cal source and integrating sphere in place of Z.

Example of cal source and integrating sphere components.

Source: Patel, S., et al. (2019)

The Project

- As noted, the current method and source for SVS calibration could be improved through use of a high flux broadband source (or sources) and simplification (or elimination) of complex correction procedures.
- Therefore, goals for this work in progress include the following:
  - Improve calibration techniques for optical spectroscopy on Z
    - Expand source spectral range and optimize radiance
    - Simplify method to reduce error and processing time
    - Design calibration setup integrating new source and optics for easy use
- Work thus far has focused on identification and evaluation of LED sources. Plots below illustrate the current spectral limitations discussed with the tungsten source (left) and potential spectral coverage available with LEDs (right).

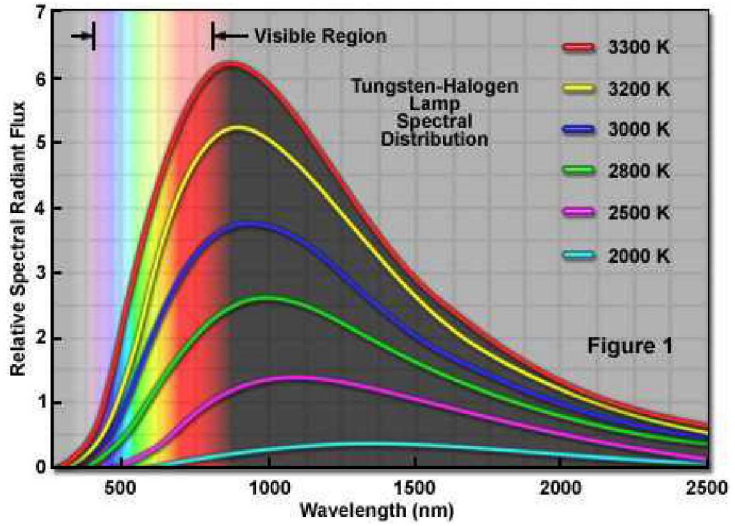

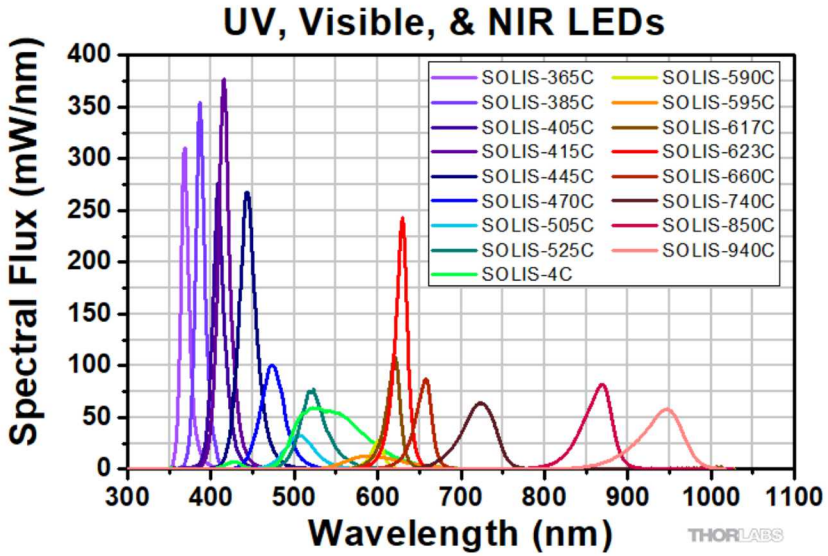

Sources: (left) http://zeiss-campus.magnet.fsu.edu/articles/lightsources/tungstenhalogen.html (right) https://www.thorlabs.com/newgrouppage9.cfm?objectgroup_id=8986

The Project

- While many turnkey LED products are available, very few provide flux levels in the needed range, but investigation is on-going using any commercially available performance data.
- The ideal source is broadly incoherent, and continuous wave with high radiance capability.
- Desired spectral radiance at sphere aperture is approximately 10^5 W/m^2/sr/nm.
- Matlab codes are in development to ease investigation calculations for radiance capability and design parameters.
- Two examples of potential sources are provided below. The Thorlabs product on the left, is one of a series of high power LEDs available (flux plot on previous slide). Preliminary calculations suggest that Solis_445C provides the greatest power (~7 W) in the lower spectral range. The Gamma Scientific product on the right is a calibrated broadband source but seemingly lacks usable output.
- During this investigation, comparison of other source types are planned, such as laser, to verify cal set up optimization.

Sources: (left) https://www.thorlabs.com/newgrouppage9.cfm?objectgroup_id=8986 (right) https://www.gamma-sci.com/products/rs-7-1-benchtop-uniform-light-source

Summary

- The onset of WWII and the Manhattan project produced a distinct group of engineers at Los Alamos National Labs, referred to as the Z-division. While continuing to support nuclear research, these engineers separated from LANL and became Sandia Corporation, located in Albuquerque, by 1949.
- Sandia experienced massive growth throughout the 1950s and greatly advanced pulsed-power technology with the construction of HERMES for gamma ray studies in 1965. Continued innovations lead to the PBFA II accelerator in 1986, the world's most powerful x-ray source. By 1996, PBFA II was rebuilt and became Z.
- The Z machine at Sandia remains the world's largest pulsed-power accelerator (33 m diameter), capable of storing up to 22 MJ of energy and releasing it within nanoseconds. Peak power and current is in the range of 80 TW and 30 MA. Target materials in the center chamber are compressed under Mbar pressures, and primary areas of research include: x-ray radiation effects, materials studies, and fusion containment.
- Streaked Visible Spectroscopy (SVS) is the primary method utilized for optical spectroscopy on Z. A streak camera captures intensity, wavelength, and time information, which is used to determine plasma parameters such as species, particle temperatures, and densities. SVS is used on many Z experiments as part of a diagnostic suite including B-dot and VISAR, for current and velocity measurements respectively.
- Four highlighted experiments provide examples of using SVS data. Spectra of shocked samples, spectra of plasmas, verification of magnetic fields, and determination of peak radiance levels are a few results form SVS.
- Due to an applied magnetic field, Zeeman/Paschen-Back splitting is commonly observed through SVS. Stark effect can be used to measure electron densities but remains a work in progress to measure electric fields.
- Calibration of SVS entails using a tungsten source which requires a complex correction procedure and is limited in lower spectral range. Focus of the assigned project is to improve the optical calibration technique including identification, procedure, and integration of a new source with high flux and broad spectral range.

References

1. Johnson, L. (1997). Sandia national laboratories: a history of exceptional service in the national interest. Sandia National Laboratories.
2. Van Arsdall, A., & Sandia National Laboratories. (2007). Pulsed power at sandia national laboratories : the first forty years. Sandia National Laboratories.
3. Sinars, D. B., et al. (2020). Review of pulsed power-driven high energy density physics research on Z at Sandia. Physics of Plasmas, 27(7), 070501–070501.
4. National Nuclear Security Administration. About NNSA. Retrieved from https://www.energy.gov/nnsa/about-nnsa
5. Schwarzschild, B. (2003). Inertial-confinement fusion driven by pulsed power yields thermonuclear neutrons. Physics Today, 56(7), 19–21.
6. Shwarz, J., et al. (2017). Z-Backlighter: Past - Present - Future. [Power Point]. Retrieved from Sandia Technical Library.
7. Anderson, D. et al. (2012). High-current linear-transformer-driver (LTD) science and technology. [Power Point]. Retrieved from Sandia Technical Library.
8. Savage, M. E., et al. (2007). An overview of pulse compression and power flow in the upgraded z pulsed power drive. 2007 IEEE Pulsed Power Plasma Science Conference (pp. 979–984).
9. Cooper, J. (1966). Plasma spectroscopy. Reports on Progress in Physics, 29(1), 35–130.
10. Huang, X., & Yung, Y. L. (2004). A common misunderstanding about the voigt line profile. Journal of the Atmospheric Sciences, 61(13), 1630–1632.
11. Hamamatsu Photonics K.K. (2008). Guide to streak cameras.
12. Bailey, J. E., et al. (2000). Optical spectroscopy measurements of shock waves driven by intense z-pinch radiation. Journal of Quantitative Spectroscopy and Radiative Transfer, 65(1-3), 31–42.
13. Gomez, M. R., et al. (2014). Magnetic field measurements via visible spectroscopy on the z machine. The Review of Scientific Instruments, 85(11), 11–609.
14. Gomez, M. R., et al. (2017). Experimental study of current loss and plasma formation in the z machine post-hole convolute. Physical Review Accelerators and Beams, 20(1).
15. Patel, S., Simpson, S. (2019). Active dopant optical spectroscopy via laser ablation for high resolution spectral measurements. [LDRD Report]. Sandia National Laboratories.
16. Patel, S. (2016). Optical spectroscopy and magnetic field profile measurements on the self magnetic pinch diode. [Doctoral dissertation]. University of Michigan, Ann Arbor, Michigan.